Imprints of Sea Ice, Wind Patterns, and Atmospheric Systems on Summer Water Isotope Signatures at Hercules Névé, East Antarctica

Songyi Kim[1,2], Yeongcheol Han[2], Jiwoong Chung[2], Seokhyun Ro[2,3], Jangil Moon[2], Soon Do Hur[2] and Jeonghoon Lee[1]

[1]Department of Earth Science Education, Ewha Womans University, Seoul, 03760, Republic of Korea
[2]Division of Glacier & Earth Science, Korea Polar Research Institute, Incheon, 21990, Republic of Korea
[3]Department of Ocean Sciences, Inha University, Incheon, 22212, Republic of Korea

Correspondence to: Jeonghoon Lee (jeonghoon.lee@gmail.com)

Abstract. This study investigated the influence of summer climate variability on water isotopes ($\delta^{18}O$, $\delta^{2}H$, and deuterium excess[dexc]) in a Hercules Névé ice core from Antarctica. High-resolution ERA5 reanalysis data for the austral summer months (1979–2015) were employed to evaluate the relative contributions of temperature, precipitation, wind patterns (v- and u-winds), ocean condition (sea ice concentration [SIC] and sea surface temperature [SST]), and large-scale circulation system (Amundsen Sea Low [ASL] and Zonal Wave-3 [ZW3]) to isotopic variability. The results indicated that higher temperatures and precipitation are positively associated with $\delta^{18}O$, highlighting their combined role in controlling isotopic enrichment. Wind patterns also contribute meaningfully but in a more complex way: enhanced southerly winds (positive v-wind anomalies) tend to increase $\delta^{18}O$ by transporting relatively warm, moisture-rich air from lower latitudes, whereas stronger westerly winds (positive u-wind anomalies) are associated with more depleted isotopic values, likely reflecting colder or more distant moisture sources. Additionally, the dexc showed positive correlations with SIC and negative correlations with SST, providing valuable insights into moisture source processes in the study region during austral summer. The ASL and ZW3 also emerge as key circulation features that modulate heat and moisture transport, thereby driving isotopic variability. Taken together, these findings suggest that the summer isotope record at Hercules Névé reflects not only local temperature changes but also the broader imprint of ocean–atmosphere interactions, including sea-ice variability and large-scale circulation patterns. This underscores the potential of coastal Antarctic ice cores to provide refined constraints on the coupled climate processes governing isotopic variability and to enhance paleoclimate reconstructions in this region.

1 Introduction

Water isotopes ($\delta^{18}O$ and $\delta^{2}H$) have served as crucial proxies for paleoclimatic reconstructions due to their systematic relationship with temperature, making ice cores invaluable archives of past climatic information (Dansgaard, 1964; Jouzel et al., 1997). Recent advancements, such as refined surface temperature reconstructions using advanced modeling approaches (Markle and Steig, 2022) and analyses of isotopic diffusion in snow layers for estimating past temperatures (Holme et al., 2018), highlight the progression from observational studies toward sophisticated modeling. Despite these advancements, accurately interpreting isotopic records from ice cores remains challenging, particularly due to regional variability in the temperature-isotope relationship. In polar regions, and especially across Antarctica, local climatic and atmospheric conditions significantly influence this relationship, creating spatial differences in isotopic signals (Masson-Delmotte et al., 2008; Sime et al., 2009).

Therefore, detailed regional investigations are essential for bridging these gaps in understanding and ensuring accurate interpretations of paleoclimatic conditions from ice core isotope records.

Victoria Land in East Antarctica offers unique advantages for understanding climatic processes due to its transitional position between the high interior plateau and the coastal regions. Previous research in this area has utilized ice cores from locations such as Styx Glacier, Talos Dome, Whitehall Glacier and Hercules Névé to study regional climate dynamics (Bertler et al., 2011; Emanuelsson et al., 2023; Masson-Delmotte et al., 2008; Nyamgerel et al., 2024; Sime et al., 2009; Stenni et al., 1999, 2002; Thomas et al., 2017). Each of these sites has contributed distinctive insights: Styx Glacier provides detailed records of local temperature trends (Nyamgerel et al., 2024; Thomas et al., 2017), while Talos Dome captures long-term climatic signals influenced by marine-continental air mass interactions (Frezzotti et al., 2007). Research at Whitehall Glacier has emphasized its role in documenting snow accumulation patterns and their relationship to atmospheric dynamics (Sinclair et al., 2012). These studies have collectively advanced our understanding of isotopic variability and its relationship to atmospheric processes. Among these locations, Hercules Névé is distinguished by its location near the Ross Sea, enabling it to capture isotopic signals influenced by both coastal and interior atmospheric systems. The high snow accumulation rates in this region allow for the preservation of detailed isotopic records, which are essential for investigating Antarctic climate variability and its broader global impacts (Masson-Delmotte et al., 2003; Sinclair et al., 2012).

Isotope-enabled general circulation models demonstrate that sea ice extent and concentration influence the isotopic composition of polar coastal precipitation by altering moisture source regions and transport pathways, ultimately shaping the isotopic signatures recorded in precipitation (Faber et al., 2017; Noone and Simmonds, 2004). Reduced sea ice exposes nearby open ocean areas, enhancing evaporation from local sources and typically leading to enriched $\delta^{18}O$ values due to shorter transport distances. Conversely, expanded sea ice displaces evaporation sources farther from the continent, lengthening the distillation pathway and promoting isotopic depletion. However, recent studies indicate that these relationships are not spatially or seasonally uniform, and can be modulated by regional atmospheric circulation, moisture recycling, and synoptic activity (Song et al., 2023).

The relationship between sea ice and moisture transport is shaped by various atmospheric circulation features, with the Amundsen Sea Low (ASL) being particularly influential in the Ross Sea region due to its role in directing moisture transport and modulating wind patterns (Hosking et al., 2013; Raphael et al., 2016). Another critical pattern is Zonal Wave 3 (ZW3), which is statistically associated with the distribution of air masses and precipitation in coastal Antarctica on seasonal to interannual timescales, and reflects the influence of regional circulation dynamics. (Goyal et al., 2022). While ASL and ZW3 modulate these interactions, regional cyclonic activity also contributes to shaping the isotopic composition of precipitation in coastal Antarctica. This modulation affects regional precipitation isotopes and links sea ice variability with broader atmospheric processes (Emanuelsson et al., 2023; Sinclair et al., 2013).

The Austral summer months of December, January, and February (DJF) are particularly suitable for sea ice research because of the climatic and environmental dynamics observed during this period. For example, Antarctica experiences higher solar radiation levels during DJF, leading to dynamic changes in the extent and structure of sea ice. These katabatic winds flow downslope from the interior year-round and generally intensify in winter; they drive offshore advection/divergence of coastal sea ice and are associated with coastal polynya formation. In winter such polynyas can enhance net sea-ice production through increased heat loss and subsequent freezing (Dale et al., 2020; Turner et al., 2016). These polynyas facilitate the exchange of heat and moisture between the ocean and atmosphere, influencing local and regional climate patterns (Stammerjohn et al., 2015). Additionally, higher precipitation rates in DJF lead to the greater preservation of isotopic signals, allowing for more detailed analysis of seasonal variation.

The primary objective of this study was to analyze how water isotopes in the Hercules Névé region respond to various climatic drivers during the Austral summer months. In particular, the relationship between isotopic signals and climatic factors was assessed by determining the influence of temperature, precipitation, and u- and v-wind components on isotopic variability. By focusing on climatic patterns and isotopic signals during the DJF period, it was possible to identify the impact of seasonal processes on isotope records. Accordingly, this study aims to assess whether the summer isotope signals preserved at Hercules Névé can be regarded solely as indicators of local temperature, or whether they also embody the combined influence of regional atmospheric circulation and ocean–atmosphere interactions. More specifically, the analysis focuses on (1) the extent to which $\delta^{18}O$ variability is modulated by precipitation and circulation in addition to temperature, and (2) whether d-excess can serve as a sensitive tracer of sea-ice concentration and sea surface temperature. By addressing these questions, the study contributes to a more robust interpretation of coastal Antarctic ice-core records and enhances their relevance for paleoclimate reconstruction.

2 Materials and methods

2.1 Study Area

The research area is located at Hercules Névé, Victoria Land, Antarctica, at 73°03'S, 165°25'E (Figure 1). Situated at an altitude of 2,864 m and approximately 80 km inland from the sea, the climatic conditions of this mountainous area are affected by its position near the northern edge of the Transantarctic Mountains, which strongly influence atmospheric circulation by acting as a barrier to the flow of air masses (Tewari et al., 2021). Because the interaction between the mountains and the prevailing winds generates various microclimates at Hercules Névé, it has become an area of interest for understanding the complex interactions between the local geography and climate (Maggi and Petit, 1998).

Victoria Land has long been used as a research site to study the impact of atmospheric and oceanic variability on snow accumulation and ice core records (Maggi and Petit, 1998; Nardin et al., 2020; Nyamgerel et al., 2024; Yan et al., 2021; Yang et al., 2018). This region is characterized by austral summer-dominant precipitation patterns influenced by easterly winds that bring moist air from the ocean onto the continent (Scarchilli et al., 2011). Katabatic winds descending from the East Antarctic Plateau are typically cold and extremely dry. Their dryness enhances sublimation from the snow surface, which can lead to isotopic modification of near-surface layers (Nyamgerel et al., 2024; Vihma et al., 2011). However, their impact on local temperature and the surface energy balance is not always unidirectional and may vary depending on synoptic conditions (Davrinche et al., 2024). Broader climatic drivers such as the Southern Annular Mode and sea ice variability also impact regional weather patterns and precipitation (Yang et al., 2018). Hercules Névé is thus a useful site for the analysis of how regional climate variability influences snow deposition and ice core records, which can be used to reconstruct past climate conditions. Furthermore, previous studies have reported a high snowfall rate in the surrounding area (Maggi and Petit, 1998; Nyamgerel et al., 2020; Stenni et al., 1999, 2000), making this region particularly suitable for ice core seasonal analysis.

2.2 Data Acquisition

2.2.1 Sampling and Water Isotope Data

To acquire water isotope data from Hercules Névé in northern Victoria Land, an ice core was drilled between 11 and 15 December 2015, according to the method described by Han et al. (2015). The ice core was extracted to a depth of approximately 80 m, was immediately segmented, sealed in plastic bags, logged, and packaged in insulated containers to prevent temperature fluctuations during transport to a laboratory at the Korea Polar Research Institute (KOPRI). After drilling was completed in December 2015, the Hercules Névé ice core was transported to the Korea Polar Research Institute (KOPRI), where it was stored frozen until cutting. In the second half of 2017, the core was cut into 5 cm segments in a clean laboratory environment to ensure seasonal-scale resolution.

In the laboratory, the ice core was carefully segmented into 5 cm sections based on analytical needs to assess seasonal variability, yielding approximately 2,000 segments. This segment size was selected to ensure data representativeness and ease of handling by providing a balance between resolution and sample manageability. Each segment was processed in a clean environment to prevent contamination. The ice was melted at room temperature in sealed containers to avoid isotopic fractionation via physical processes such as evaporation and sublimation. The meltwater was filtered through 0.45 μm syringe filters to remove particulates and transferred into 2 ml high-density polyethylene (HDPE) vials with airtight caps to prevent isotopic exchange with ambient air.

All samples were stored at temperatures below 4 °C and were analyzed within 12 months of preparation to ensure isotopic stability. The liquid samples were analyzed using a Picarro L2130-i water isotope analyzer, which employs cavity ring-down spectroscopy (CRDS) for high-precision measurements. The analyzed water isotope results were expressed using delta notation, as shown in Eq. (1):

$$\delta\ (‰) = \left({R_{standard}}/{R_{sample}} - 1 \right) \times 1000 \quad (1)$$

The secondary parameter deuterium excess (dexc), defined according to Dansgaard, (1964), was also determined as shown in Eq. (2):

$$\text{dexc} = \delta\, ^2H - 8 \times \delta^{18}O \quad (2)$$

The $\delta^{18}O$ and δ^2H values were measured using a Picarro L2130-i water isotope analyzer. Measurement precision was ± 0.07 ‰ for $\delta^{18}O$ and ± 0.1 ‰ for δ^2H, based on long-term repeated measurements of laboratory standards conducted over multiple years. The measurements were calibrated using the international standards VSMOW, Greenland Ice Sheet Precipitation (GISP), and Standard Light Antarctic Precipitation (SLAP), as well as the laboratory standard RS (–34.69 ± 0.07 ‰ for $\delta^{18}O$, –272.4 ± 0.6 ‰ for δ^2H). The measurements followed the internal analytical protocol used at KOPRI, as described in (Kim et al., 2022). Each sample was injected 12–15 times, and the average of the final 5 measurements was used to ensure thermal and instrumental stability. International reference waters (VSMOW, SLAP, GISP) were measured every ~100 samples for calibration, and laboratory reference waters were measured after every 10 unknowns to monitor analytical consistency. This procedure ensured high precision and long-term stability of the isotope measurements.

2.2.2 Utilization of ERA5 Data and ZW3 Data

In this study, we utilized ERA5 reanalysis data provided by the European Centre for Medium-Range Weather Forecasts (ECMWF, covered on a 31 km grid) (Hersbach et al., 2020). ERA5 has been widely validated for use in Antarctica due to its high temporal and spatial resolution and strong correlation with observational data (Tetzner et al., 2019). During the ice core sampling campaign, an automatic weather station (AWS) was installed at the Hercules Névé site to collect local meteorological data over the span of one year. The AWS recorded air temperature, wind speed, wind direction, relative humidity, and atmospheric pressure at regular intervals. To assess the accuracy of reanalysis data in representing local atmospheric conditions, the AWS dataset was compared with ERA5 outputs, focusing on temperature and wind variables (Figures S1 and S2). ERA5 reproduces general patterns in temperature and wind direction well. However, it tends to overestimate summer (DJF) temperatures relative to AWS, as shown by the DJF AWS–ERA5 comparison using a York regression analysis (Figure S1(C); R^2=0.57). Despite this warm bias, ERA5 provides consistent temporal coverage from 1979 to 2015, making it suitable for evaluating interannual climate–isotope relationships in this remote region. Wind direction and speed distributions also show notable differences between AWS and ERA5 (Figure S2). ERA5 indicates a dominant southerly to southeasterly wind regime during DJF, in line with broader synoptic circulation over the Ross Sea. In contrast, AWS data show more variable wind directions and stronger speeds, likely reflecting local topographic effects and boundary-layer dynamics.

These differences highlight the complementary nature of AWS and ERA5: while AWS offers fine-scale, site-specific observations, ERA5 captures broader regional-scale patterns relevant to climate–isotope interpretations. We also used the monthly ZW3 index from Goyal et al. (2022), which is derived from ERA5 sea level pressure fields and offers higher temporal and spatial resolution than previous datasets. ZW3 is characterized by three large-scale ridges and troughs in the mid-latitudes of the Southern Hemisphere, influencing atmospheric circulation and sea ice distribution around Antarctica (Goyal et al., 2022; Raphael, 2007). The inclusion of the new ZW3 data allows for a more detailed assessment of its impact on the climatic conditions at Hercules Névé via isotopic signatures.

2.3 Data Processing

2.3.1 Age Dating

Manual layer counting is widely used for the age dating of ice cores, with the identification of annual layers relying on variation in proxies such as stable water isotopes ($\delta^{18}O$, $\delta^{2}H$, and dexc), ion concentrations, dust deposition, and electrical conductivity method (ECM) (Johnsen et al., 2001; Masson-Delmotte et al., 2003; Sigl et al., 2016; Sinclair et al., 2012). Previous studies have demonstrated that, in regions with abundant snowfall, particularly along coastal areas, water isotope signals are well-preserved and exhibit clear seasonal cycles, allowing for the precise manual counting of annual layers. Seasonal variation in $\delta^{18}O$, $\delta^{2}H$, and dexc from the Hercules Névé ice core, characterized by higher $\delta^{18}O$ and $\delta^{2}H$ values during warmer months and lower values during colder periods, were thus used to establish annual layers for age dating (Figure 2B–D). This method provides a high-resolution age model based on stable water isotope variation, which can be linked to specific years and climatic events.

Radioactive isotopes resulting from atmospheric nuclear testing, such as plutonium-239 (^{239}Pu) and tritium, can be utilized to validate the accuracy of the manual layer counting method (Hwang et al., 2019; Stenni et al., 1999). In this study, ^{239}Pu concentrations were measured at various depths within the Hercules Névé ice core, and ^{239}Pu peaks corresponding to known periods of atmospheric nuclear testing in the late 1950s and early 1960s were employed as absolute time markers (Figure 2A). By matching these peaks with the historical records for nuclear testing, we confirmed the age of specific layers and validated the annual layer counting method. The uncertainty for the age dating of the ice core was assumed to be less than a year.

In this study, we successfully determined the ice core chronology back to the 1950s, reaching a depth of approximately 25 m. For isotopic and climate analysis, we used the top 16 m of the core, which represents roughly 40 years of accumulation (highlighted in grey in Figure 2). Clear seasonal cycles in $\delta^{18}O$ and d-excess enabled manual annual layer counting to construct a high-resolution age–depth model. The estimated mean annual snowfall over this period was 204.5 kg m^{-2} y^{-1} ± 54.5. Within each annually dated layer, each sample point (typically 5–15 per year) was assigned a fractional year value based on its relative depth position. To assign calendar months, the $\delta^{18}O$ maximum within each year was used as an anchor point and fixed to January, representing the midpoint of the austral summer. All other sample positions were then linearly interpolated across the year. While this approach assumes that $\delta^{18}O$ peaks reflect summer accumulation, the use of DJF averages, centered around the $\delta^{18}O$ maximum and spanning three months, minimizes sensitivity to short-term variability in peak timing. This interpolation allowed for monthly-resolved isotope estimates, including months not directly sampled. From this monthly-interpolated series, DJF values were extracted and averaged to produce an annual DJF $\delta^{18}O$ time series from 1979 to 2015. This time series was subsequently used in correlation analyses with ERA5-derived temperature, precipitation, and wind data to interpret climatic influences on isotopic variability.

2.3.2 Statistical Analysis

We applied multiple statistical methods to evaluate the relationship between water isotopes and various climatic drivers in the Hercules Névé region. All climate variables were derived from the ERA5 reanalysis dataset (Hersbach et al., 2020) for the period 1979–2015, including 2 m air temperature, total precipitation, u- and v-wind components, and sea ice concentration. Spatial correlation analysis was performed between the $\delta^{18}O$ time series and gridded ERA5 climate fields to identify dominant spatial patterns. Pearson correlation coefficients were computed on a seasonal (DJF) basis to assess spatially coherent relationships (e.g., Sime et al., 2009; Thomas et al., 2017). To examine large-scale circulation drivers, we used a monthly Zonal Wave 3 (ZW3) index developed by Goyal et al. (2022), which captures hemispheric wave structure more accurately than earlier indices. We also used monthly ASL strength (central pressure), latitude, and longitude provided by the British Antarctic Survey, based on the method of Hosking et al. (2013), where the ASL is identified as the climatological low in mean sea level pressure over the Amundsen Sea.

These three ASL parameters were subjected to Principal Component Analysis (PCA) to identify coupled spatial–intensity modes of ASL variability (Coggins and McDonald, 2015). The resulting PCs were correlated with $\delta^{18}O$ to determine which modes had the strongest association with isotopic variability. To investigate broader circulation patterns, we performed Empirical Orthogonal Function (EOF) analysis of 500 hPa geopotential height fields for DJF, following standard methods (e.g., Raphael et al., 2016; Clem et al., 2017). The corresponding principal components were used to interpret SAM- and ZW3-like structures and their association with $\delta^{18}O$ variability. Lastly, to assess atmospheric moisture pathways, we used the HYSPLIT model (Stein et al., 2015) to compute 7-day backward trajectories arriving at Hercules Névé. Cluster analysis was conducted for the five strongest and five weakest ASL summers, as identified from the ASL strength data, to visualize dominant transport regimes and shifts in source regions of moisture.

To assess the signal-to-noise ratio and test whether the $\delta^{18}O$ record contains a preserved seasonal signal, we performed a Lomb–Scargle periodogram analysis. As shown in Figure S3, the spectrum exhibits a statistically significant peak at 1/year ($p < 0.05$), indicating that the time series retains a robust seasonal (annual) cycle. This result supports the use of DJF-averaged isotope values for climate correlation analysis and justifies the seasonal aggregation approach used throughout this study. To check whether post-depositional processes bias our summer signal, we evaluated the DJF $\delta^{18}O$–d-excess relationship following Casado et al. (2021). In this framework, negative relationships imply substantial modification, whereas positive relationships suggest minimal alteration. For Hercules Névé, the diagnostic outcome is positive in DJF ($r = 0.51$), indicating limited post-depositional modification.

3 Results

3.1 Water Isotope Records in the Ice Core from Hercules Névé

Figure 2 presents the water isotope data for the 1979–2015 period from Hercules Névé. The $\delta^{18}O$ values in the Hercules Névé ice core ranged from –42.29 ‰ to –29.67 ‰, with a standard deviation of 1.69 ‰, while those for δ^2H ranged from –334.5 ‰ to –226.1 ‰, with a standard deviation of 11.75 ‰. Several other near-coastal ice cores have been studied in the broader Victoria Land region, including Styx–M, Whitehall Glacier, and Talos Dome, each offering different altitudinal and geographical contexts. A summary of isotope statistics and core characteristics for these sites is provided in Table S1.

Using the annual mean $\delta^{18}O$ and δ^2H in Hercules Névé core, we derived a local meteoric water line (LMWL) with a slope of 8 and an intercept of 8.2 (R^2=0.99). While there slope and intercept are higher than those of the Antarctica meteoric water line (AMWL, slope = 7.75 and intercept = –4.93 Masson-Delmotte et al., 2008), they are similar to the global meteoric water line (GMWL, slope = 8 and intercept = 10; Craig, 1961). The result indicates that the Hercules Névé region, being relatively close to the coast, experiences moisture conditions more akin to oceanic sites, possibly leading to a steeper $\delta^{18}O$–δ^2H relationship (Fernandoy et al., 2010; Goursaud et al., 2018; Nyamgerel et al., 2024).

Seasonally, the $\delta^{18}O$-δ^2H relationship in the Hercules Névé core range from 8 to 8.3 and 7.8 to 18 (Figure S4). Notably, the austral summer, the slope is 8 and the intercept is 7.8, matching closely with the annual mean LMWL. This suggests that isotopic signals during summer precipitation are more likely to reflect the underlying temperature–isotope relationship, with minimal post-depositional alteration. ERA5 reanalysis data from 1979–2015 show that precipitation minus evaporation during DJF accounts for approximately 23–40% (mean 35%, standard deviation 4%) of the annual total. While DJF does not dominate the annual accumulation in terms of volume, it occurs under conditions of relatively frequent snowfall, warmer atmospheric temperatures, and higher moisture flux from open ocean areas due to reduced sea ice extent. Such conditions may enhance the direct imprint of summer climatic signals into the isotopic composition of snow, making the DJF season particularly valuable for interpreting isotope–climate relationships in coastal Antarctica. To further assess whether this seasonal signal was preserved without significant isotopic smoothing, we empirically estimated the diffusion length from the $\delta^{18}O$ time series using a spectral fitting approach(Münch et al., 2016). The resulting diffusion length of approximately 6 cm is comparable to our 5 cm sampling interval, indicating that seasonal variability is well resolved at this resolution.

3.2 Impact of Summer Climate Patterns on Water Isotope in the Antarctic Hercules Névé

Using ERA5 climate reanalysis data from 1979 to 2015, we conducted a spatial correlation analysis to examine how temperature, precipitation, and the v- and u-wind components relate to $\delta^{18}O$ variations during the austral summer in the Hercules Névé region (Figure 3). When considering annual mean temperature (1979–2015), $\delta^{18}O$ shows a weak correlation ($r = 0.13$). This modest relationship likely arises from the confluence of multiple processes that obscure a straightforward isotopic–thermal link: varying moisture sources (Masson-Delmotte et al., 2008; Noone and Simmonds, 2004), strong synoptic variability associated with the Ross Sea (Schlosser et al., 2016), the seasonality of precipitation events (Casado et al., 2018), and post-depositional modifications of the snowpack (Casado et al., 2021; Kanthanathan et al., 2020). Such processes dilute the climate signal in the annually averaged isotope record, which is a point of caution for paleoclimate reconstructions based solely on mean annual signatures (Laepple et al., 2025). By contrast, during the austral summer, a more pronounced correlation was observed, with a correlation coefficient of 0.32 ($p < 0.05$) and a slope of 0.59 ‰ °C^{-1}. Although slightly lower than the Styx site (0.66 ‰ °C^{-1}; Nyamgerel et al., 2024), this summer slope is comparable to other East Antarctic locations such as Whitehall Glacier (0.62 ‰ °C^{-1}; Sinclair et al., 2012), Taylor Dome (0.50 ‰ °C^{-1}; Steig et al., 2000) and Talos Dome (0.60 ‰ °C^{-1}; Stenni et al., 2002) (Figure S5). Such agreement indicates that the isotope–temperature scaling in Hercules Névé is regionally coherent, despite different topographic settings and moisture transport histories. It also highlights the necessity of seasonal discrimination, while annual values are confounded, summer months preserve the most direct temperature signature (Sinclair et al., 2013).

Several factors may account for this stronger summer correlation: (1) reduced post-depositional processes in warmer conditions, (2) simplified moisture transport pathways, and (3) a higher frequency of precipitation events, leading to more direct incorporation of local climatic signals into the ice. These mechanisms imply that $\delta^{18}O$ in summer snowfall is a more directly associated by surface air temperature. Precipitation shows positive correlation with $\delta^{18}O$ during summer (r=0.6; Figure 3B), exceeding its annual mean correlation (r=0.3, not shown). This pattern suggests that precipitation in coastal Antarctica is often isotopically enriched during periods of heavy snowfall, reflecting moisture sourced from the nearby ocean (Servettaz et al., 2020 and Jackson et al., 2023).

Regarding wind components, the austral summer v-wind (southerly) and u-wind (westerly) are generally negative values, indicating predominant southerly and westerly winds flows. A positive correlation was observed between $\delta^{18}O$ and v-wind, suggesting that stronger southerly winds are associated with higher $\delta^{18}O$ values (Figure 3C). A positive $\delta^{18}O$ correlation with the v-wind (southerly) may seem counterintuitive in a polar context, but it reflects that stronger southerly advection enhances the inland penetration of mixed continental–oceanic air masses with higher isotopic content (Clem et al., 2017; Noone and Simmonds, 2004). Conversely, $\delta^{18}O$ is negatively correlated with the u-wind (Figure 3D), suggesting that more intense westerly winds bring colder, isotopically depleted air. These negative correlation with the u-wind underscores the role of intensified westerlies in delivering colder, isotopically depleted air from marine sectors west of the Ross Embayment(Markle et al., 2012). There results underscore the dynamic interplay between temperature, precipitation, and wind directions, all of which collectively modulated $\delta^{18}O$ variations in the Hercules Névé region.

During DJF, the Hercules Névé ice core record shows a clear co-variation between dexc and local ocean-ice conditions. When SIC is higher, dexc is generally higher, and when SST is higher, dexc is generally lower (Fig. 4A, B). Taken together with the $\delta^{18}O$–climate associations described above, this DJF dexc pattern suggests that summertime isotopic variability at Hercules Névé, located near the Ross Sea, is most closely related to local ocean–ice conditions and polynya-influenced moisture sources. This highlights that not only temperature and precipitation but also moisture source variability has a discernible influence on the isotopic signal, reinforcing the value of summer snowfall as a recorder of regional climate (Noone and Simmonds, 2002; Risi et al., 2010; Uemura et al., 2008). In summary, the combination of temperature, precipitation, and wind patterns during austral summer exerts a marked influence on $\delta^{18}O$. Such findings provide a framework for interpreting how coastal Antarctic ice cores can record regional climatic conditions, highlighting the importance of focusing on the season (DJF) that captures a clearer signal of local temperature and marine moisture influx.

4. Discussion

4.1. Relationship between the dexc and SIC/SST during the DJF Period

The Hercules Névé record reveals a pronounced positive correlation between summer sea-ice concentration (SIC) in the Ross Sea and dexc (Figure 4A). This association can be understood through the interplay of katabatic winds, sea-ice extent, and polynya processes (Dale et al., 2020; Turner et al., 2016). Under high SIC conditions, katabatic forcing drives coastal divergence, promoting the persistence of polynyas along the ice edge. Evaporation over these open polynyas imparts low initial d-excess values due to kinetic fractionation (Merlivat and Jouzel, 1979). However, subsequent mixing with continental air masses, typically enriched in dexc, augments the net isotopic composition of snowfall. At the same time, the extensive sea-ice cover serves as a barrier that suppresses vapor inflow from distant depleted sources, further amplifying the local dominance of relatively enriched, mixed air masses. The result is an overall elevation of d-excess under higher SIC conditions.

High SIC conditions are associated with the occurrence of coastal polynya, which increase local evaporation. While evaporation over polynya can produce low dexc vapor due to kinetic fractionation (Merlivat and Jouzel, 1979), mixing continental air masses–often enriched in dexc–may raise the resultant dexc observed in the precipitation (Noone and Simmonds, 2004). Moreover, higher SIC is linked to a reduced contribution from distant oceanic sources, which typically supply more ^{18}O-depleted vapor (Uemura et al., 2008). As a result, polynya-influenced and continental air masses become more prominent in the regional isotopic composition, associated with higher dexc. Such a mechanism is consistent with previous observations in polar regions where local sea-ice dynamics modulate isotopic signals (Kurosaki et al., 2020). In contrast, lower SIC in summer exposes a larger open-sea area, thereby enhancing kinetic fractionation and resulting in lower dexc (Bertler et al., 2018; Kurosaki et al., 2020). These contrasting processes underscore the importance of local moisture source variability in controlling isotopic signatures in Antarctic coastal regions.

The relationship between dexc and SST further complicates interpretation. Theory anticipates a positive SST–dexc linkage based on fractionation dynamics (Gat et al., 2003; Merlivat and Jouzel, 1979). However, our results reveal a negative correlation between dexc and SST (Figure 4B), which differs from the expected positive relationship (Merlivat and Jouzel, 1979). We hypothesize that complex ocean–atmosphere interactions in polynya regions, where sea-ice dynamics, variable SST, and atmospheric circulation converge, modify the typical SST–d-excess linkage. Further numerical modeling that includes both SST and humidity variability would be necessary to elucidate these processes more precisely (Pfahl and Sodemann, 2014; Uemura et al., 2008). These findings carry two important implications: (1) coastal Antarctic ice core d-excess provides a sensitive proxy for sea-ice extent and local air–sea coupling rather than open-ocean temperature, and (2) reconstructions using d-excess must account for the dominance of polynya processes in regions such as the Ross Sea. Further modeling that jointly considers SST variability, sea-ice fraction, and boundary-layer humidity would be essential to disentangle their intertwined effects on isotopic composition.

4.2 Influence of the ASL on Water Isotopes and Wind Patterns

The ASL has a profound impact on both δ^{18}O variability and local wind dynamics in the Ross Sea and Victoria Land (Coggins and McDonald, 2015; Turner et al., 2013). In this study, we find a significant negative correlation between the mean sea level pressure related to the ASL and δ^{18}O values in the Hercules Névé region (Figure 5A). When the ASL intensifies (i.e., its central pressure drops), cold and dry air from the Antarctic continent tends to intrude into the Hercules Névé region, which is associated with more deplete δ^{18}O in precipitation (Emanuelsson et al., 2023). This agrees with prior findings linking a stronger ASL with enhanced cold-air advection and lowered isotopic content of snowfall (Hosking et al., 2013; Raphael et al., 2019). Wind fields also play a pivotal role in isotopic dynamics. As discussed in Section 3.2, δ^{18}O exhibits a positive correlation with the v-wind (southerly) but a negative correlation with the u-wind (westerly), which reflects the advection of relatively warm/moist versus cold/dry air (Figure 5C–D; Clem et al., 2017).

To further characterize ASL behavior, we conducted a PCA using DJF ASL strength (actual central pressure), latitude, and longitude (Hosking et al., 2013). The first three principal components (PCs) explained 100% of the variance (PC1: 57.7%, PC2: 31.2%, PC3: 11.2%) (Figure 6A). PC1 reflects a general displacement toward a stronger, poleward, and eastward ASL but is only weakly associated with $\delta^{18}O$ ($r = 0.15$). PC2 captures a zonal shift with moderate association ($r = 0.27$), while PC3, though explaining the least variance, exhibits the strongest negative correlation with $\delta^{18}O$ ($r = -0.34$) (Figure 6B). The loadings for each variable (Table 1) indicate that PC3 is primarily characterized by a southward shift in ASL position, combined with increased central pressure and slight eastward displacement. This coupled ASL pattern appears to be notably associated with changes in the isotopic signature at Hercules Névé, possibly reflecting modified moisture transport pathways. Figure 7 presents the results of HYSPLIT back-trajectory cluster analysis for summers with the strongest and weakest ASL, highlighting distinct moisture transport pathways. During summers with intensified ASL (deeper central pressure), the model demonstrates that most moisture is delivered via meridional transport from the Antarctic interior and the Ross Ice Shelf, resulting in longer continental air mass trajectories. These pathways are associated with colder, isotopically depleted precipitation and elevated d-excess, consistent with the dominance of inland and shelf moisture sources.

In contrast, periods of diminished ASL show an increased proportion of zonal, ocean-originating trajectories, particularly from the Amundsen Sea sector and lower-latitude open waters. These pathways favor the transport of relatively warm, isotopically enriched air and lower d-excess values, reflecting a greater contribution of oceanic vapor. This shift underscores the role of large-scale circulation variability in mediating both surface climate and the isotopic imprint preserved in the Hercules Névé ice core. Collectively, these findings indicate that ASL variability is statistically associated with both pressure-related advection and wind-driven changes in regional circulation. Notably, although PC3 explains only 11% of the total variance, it exhibits a statistically significant negative correlation with $\delta^{18}O$, highlighting that structural shifts in ASL circulation importantly influence isotope variability in coastal Antarctica.

4.3. Relationship between ZW3 and Water Isotopes

A significant positive correlation was identified between the DJF seasonal mean strength of ZW3 and $\delta^{18}O$ ($r=0.47$, $p<0.01$) in the Hercules Névé region based on interannual values from 1979 to 2015. The ZW3 index used here was obtained from Goyal et al. (2022) and represents monthly variability in the hemispheric wave-3 structure, which we averaged over DJF to align with the period of isotopic signal accumulation in the snowpack. To examine whether broader atmospheric circulation patterns such as the Southern Annular Mode (SAM) could be influencing $\delta^{18}O$, we performed a correlation analysis using the principal components derived from an EOF analysis of 500 hPa geopotential height fields during DJF from ERA5. The first mode (EOF1), associated with SAM, showed no significant relationship with $\delta^{18}O$ ($r = 0.09$, $p = 0.58$), whereas the second mode (EOF2), consistent with ASL–ZW3 variability, had a statistically significant negative correlation ($r = -0.44$, $p < 0.01$). These results suggest that regional wave activity (ZW3) and pressure anomalies (ASL) are more closely associated with $\delta^{18}O$ variability in this region than hemispheric SAM variability.

ZW3 is linked to changes in meridional airflow patterns; its intensification coincides with more frequent advection of warm, isotopically enriched air masses toward the Ross Sea, which is associated with higher $\delta^{18}O$ values (Raphael, 2007). While the amplitude of ZW3 strength showed a moderately related to $\delta^{18}O$, the phase of this wave did not exhibit significant influence, indicating that wave amplitude rather than longitudinal displacement is more relevant for isotope variability at this site. The interaction between ZW3 and the ASL introduces additional complexity. Enhanced ZW3 activity is often accompanied by increased ASL intensity (Cohen et al., 2013), which can coincide with southward transport of cold, dry continental air, partially offsetting the warming influence of ZW3. This dynamic interplay suggests that $\delta^{18}O$ variability at Hercules Névé may represent a net balance between warm marine and cold continental air mass effects, both associated with the coupled ZW3–ASL system (Hosking et al., 2013; Turner et al., 2013). These findings highlight the importance of considering regional atmospheric wave activity and its coupling with local pressure systems when interpreting isotopic records. Further investigation into the phase relationships and the relative contributions of competing air masses would be essential to fully elucidate the mechanisms controlling isotope variability in this sector of Antarctica.

5. Conclusion

This study analyzed a Hercules Névé ice core to examine the factors associated with water isotope composition in eastern Antarctica. By investigating the upper 15 m of the 80-m ice core, we identified clear seasonal variation in the isotopic composition, allowing for a high-resolution reconstruction of approximately 40 years of ice accumulation. This chronology enabled us to trace changes in climate patterns during this period. We focused on the summer months (DJF), which are important for understanding polynya formation and the atmospheric processes linked to these features. Our results indicate that variations in water isotopes, particularly $\delta^{18}O$, are most closely associated with a combination of temperature, precipitation, and wind patterns, with additional associations involving atmospheric pressure systems such as the ASL and ZW3.

Southerly winds were associated with enriched $\delta^{18}O$ values, while westerly winds were linked to relatively depleted $\delta^{18}O$ values. This pattern highlights the complex relationships between atmospheric dynamics and isotopic composition, where wind direction and intensity may coincide with differences in local climate conditions. The dexc record from the ice core was positively associated with SIC and negatively associated with SST, which is consistent with katabatic winds and polynya activity near the Ross Sea coastal sector. The intensity of Antarctic winds and the extent of sea ice concentration were both linked to precipitation characteristics in the study area, suggesting a connection with local climate variability.

The effects of the ASL and ZW3 were also evident in their association with atmospheric circulation and isotope variability in the region. Changes in ASL intensity were associated with shifts in wind direction and strength, coinciding with changes in $\delta^{18}O$ values. ZW3 variability was linked to periods of increased transport of warm, moisture-rich air into the region, which was associated with enriched isotope composition. These observations underscore the interconnected nature of atmospheric systems and their relevance to local climate and isotopic records. However, the processes determining water isotope variability remain complex, and future work should seek to integrate additional climatic factors to improve understanding of their combined effects on ice-core isotopic records.

In summary, the variability of water isotopes in the Hercules Névé region is most closely associated with the combined effects of temperature, precipitation, wind patterns, and complex interactions with atmospheric pressure systems such as the ASL and ZW3. These findings support the interpretation that multiple atmospheric and oceanic factors should be considered when reconstructing climate and isotopic histories from Antarctic ice cores.

Acknowledgements

This research was supported by the Korea Polar Research Institute grant (PE25100) and the National Research Foundation of Korea grant funded by the Korean Government (NRF2022R1A2C3007047). This study was partially supported by Korea Institute of Marine Science & Technology Promotion (KIMST) and by the Ministry of Oceans and Fisheries (RS-2023-00256677; PM23020).

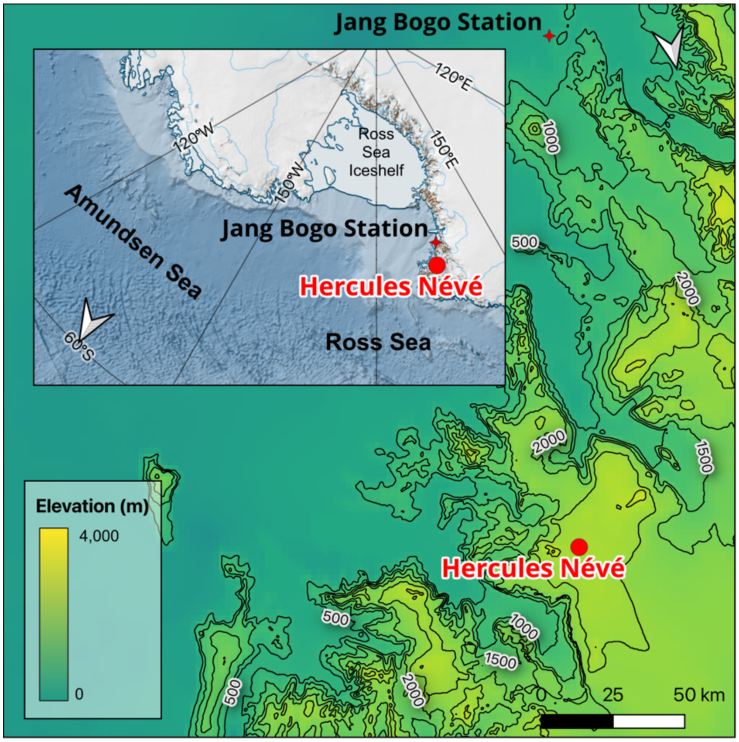

Figure 1 (A) Map of the West and East Antarctica regions showing the Ross Ice Shelf, the Ross Sea, and Hercules Névé. (B) Topographic map of Northern Victoria Land. The red circles indicate the location of the Hercules Névé ice core. The maps were created using Quantarctica 3.2 on QGIS.

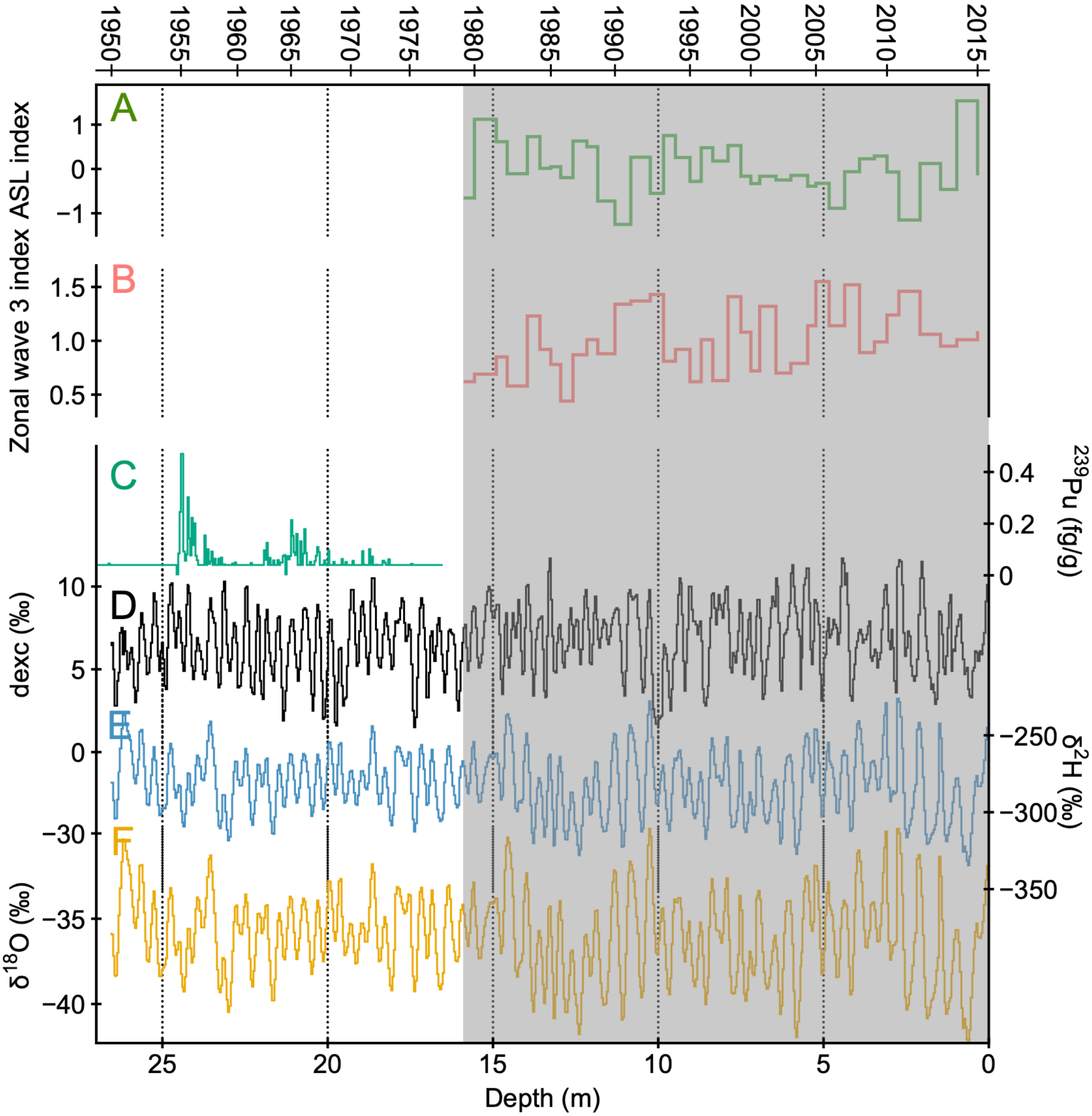

Figure 2: Depth profiles of climate indices and isotopic parameters from the surface to a depth of 26 m from the Hercules Névé ice core. Panel A represents the Amundsen Sea Low (ASL) index derived from principal component analysis (PCA) based on longitude, latitude, and strength of the ASL defined in Hosking et al. (2013), specifically displaying PC3, which showed significant correlation with isotopic data. Panel B shows the Zonal Wave 3 (ZW3) index obtained from Goyal (2022). Panel C depicts the 239Pu concentration profile for the period 1950–1975. Panels D–F illustrate water isotope measurements (dexc, δ^2H, and $\delta^{18}O$, respectively) spanning from 1950 to 2016. Data utilized for detailed analysis in this study (1979–2015) are indicated by the shaded grey region.

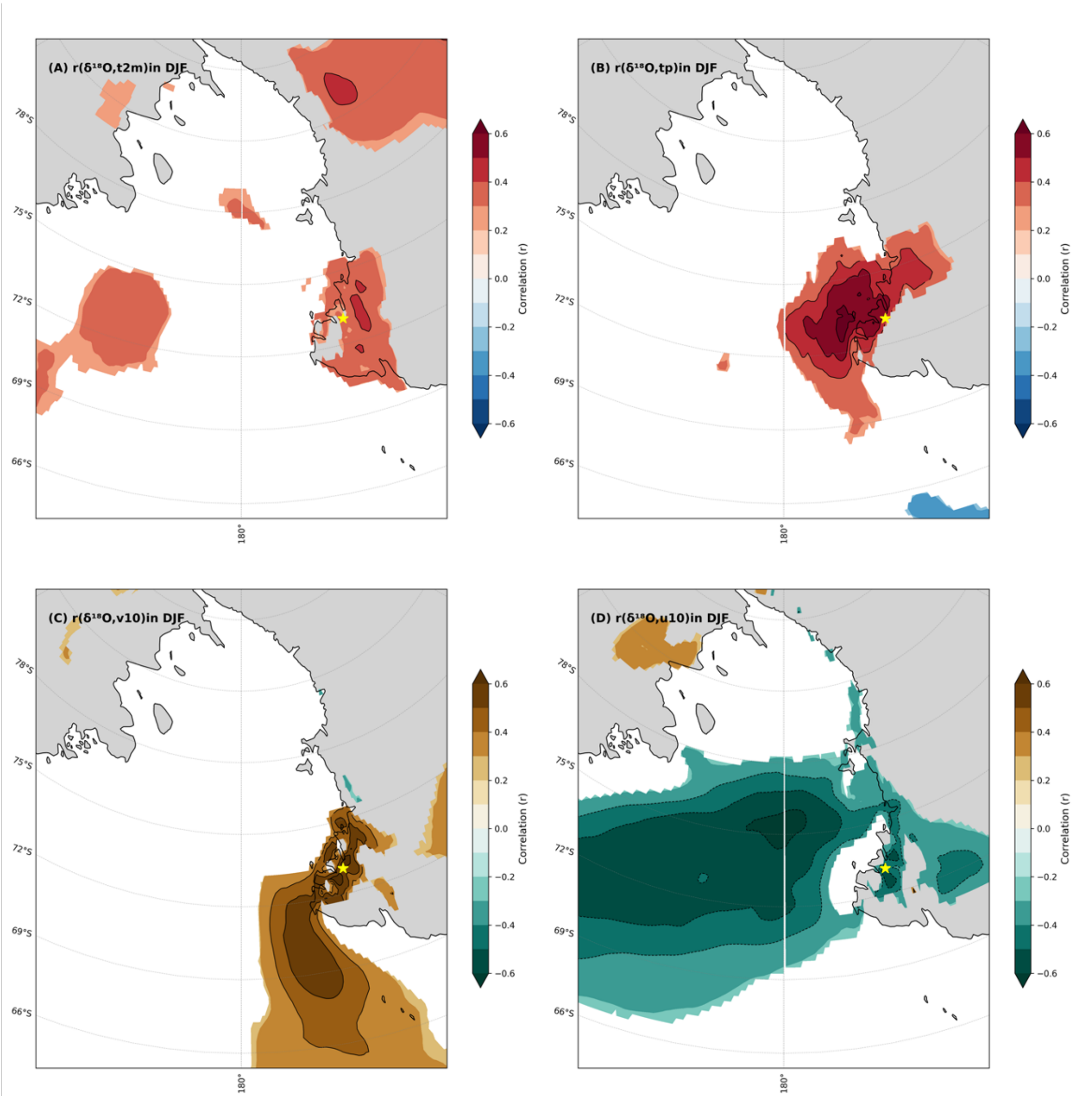

Figure 3: Spatial correlation analysis of (A) the 2 m temperature (T2m), (B) total precipitation (tp), (C) 10 m v-wind (v10), and (D) 10 m u-wind (u10) across Antarctica based on ERA5 data with $\delta^{18}O$ in HN ice core (black symbol) from 1979 to 2015 during DJF. The $p < 0.1$ confidence level is indicated by black contours.

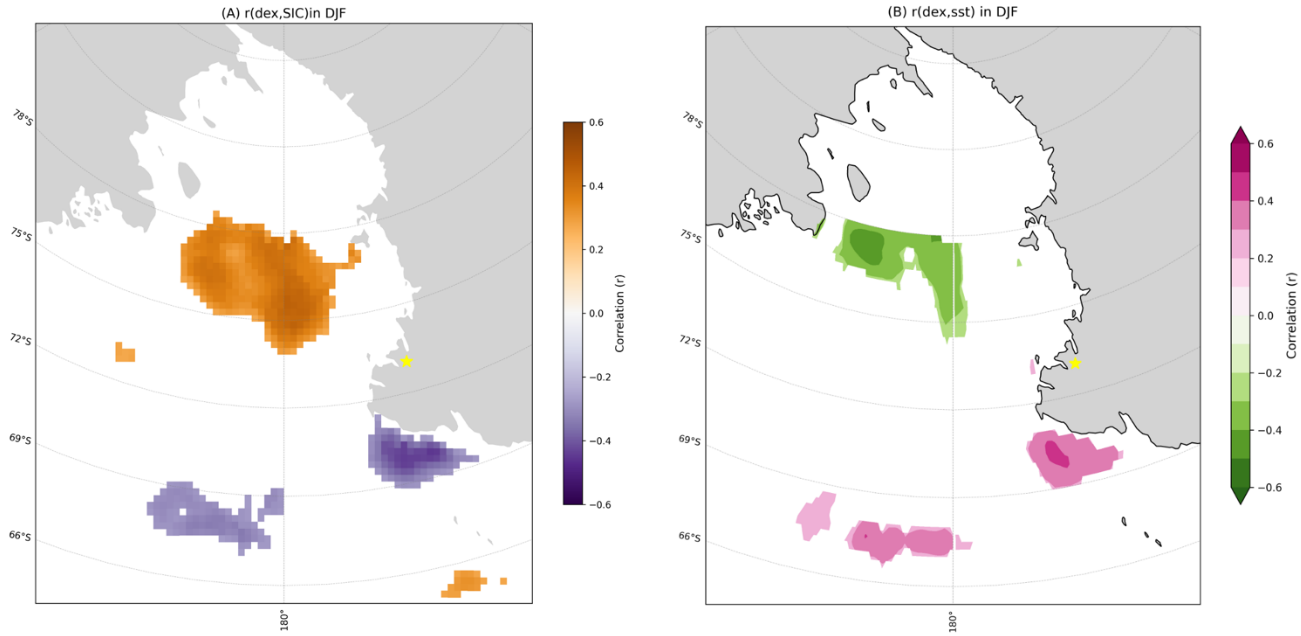

505 **Figure 4: Spatial correlation analysis results between the secondary parameter dexc from the HN ice core (black symbol) and (A) the sea ice concentration (SIC) and (B) sea surface temperature (SST) from ERA5 data during DJF for 1979–2015. The p < 0.1 confidence level is indicated by black contours.**

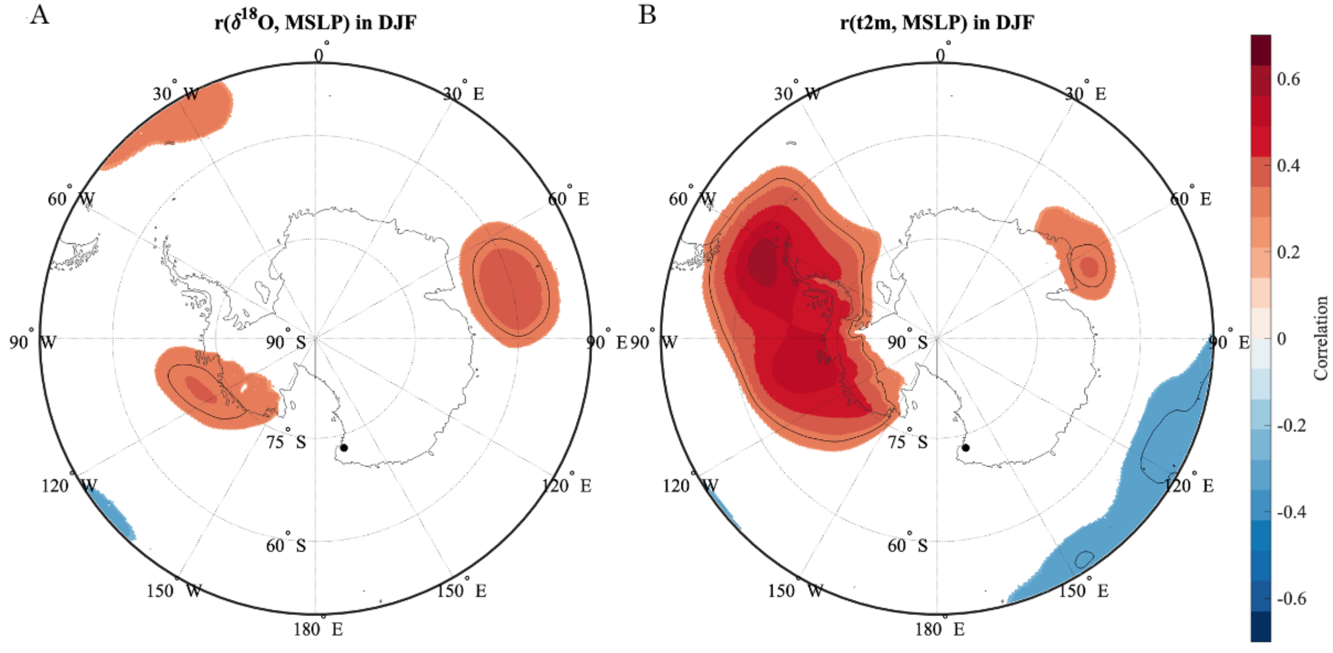

510 **Figure 5: Spatial correlation analysis for (A) δ^{18}O from the HN ice core (black symbol) and (B) the 2 m temperature (t2m) from ERA5 data with the mean sea level pressure (MSLP) from 1979 to 2015 in DJF. Contour plots are used for $p < 0.05$ and black lines for $p < 0.01$.**

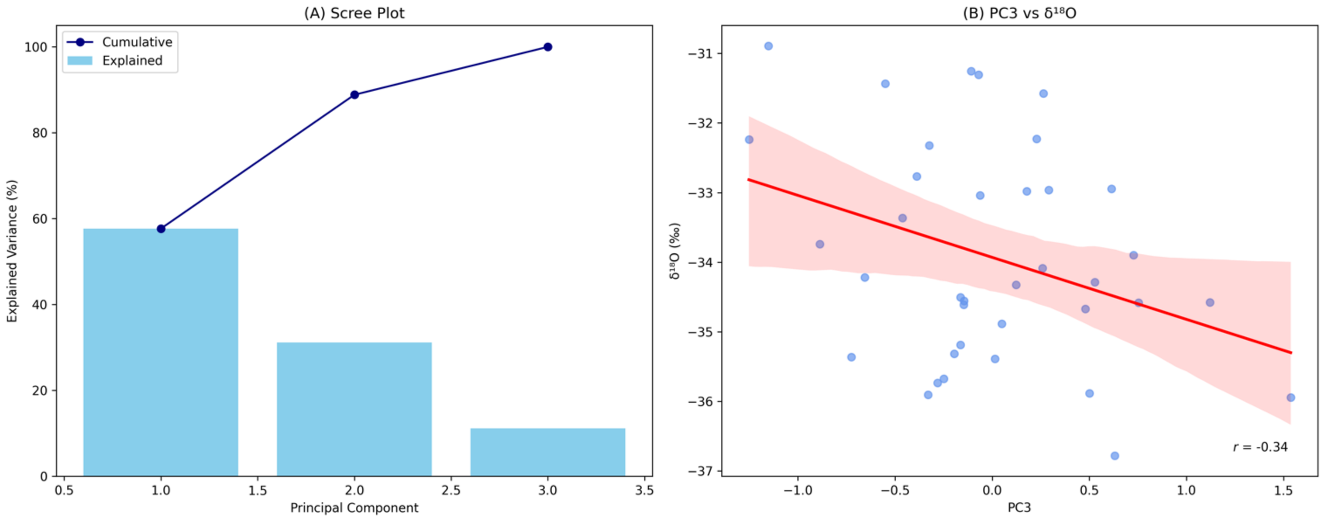

Figure 6. (A) Scree plot showing the variance explained by each principal component derived from ASL monthly variability (central pressure, latitude, and longitude) during DJF (1979–2015). (B) Scatterplot between PC3 and $\delta^{18}O$ values from Hercules Névé (r = –0.34), based on DJF-averaged data, showing the strongest correlation among all PCs.

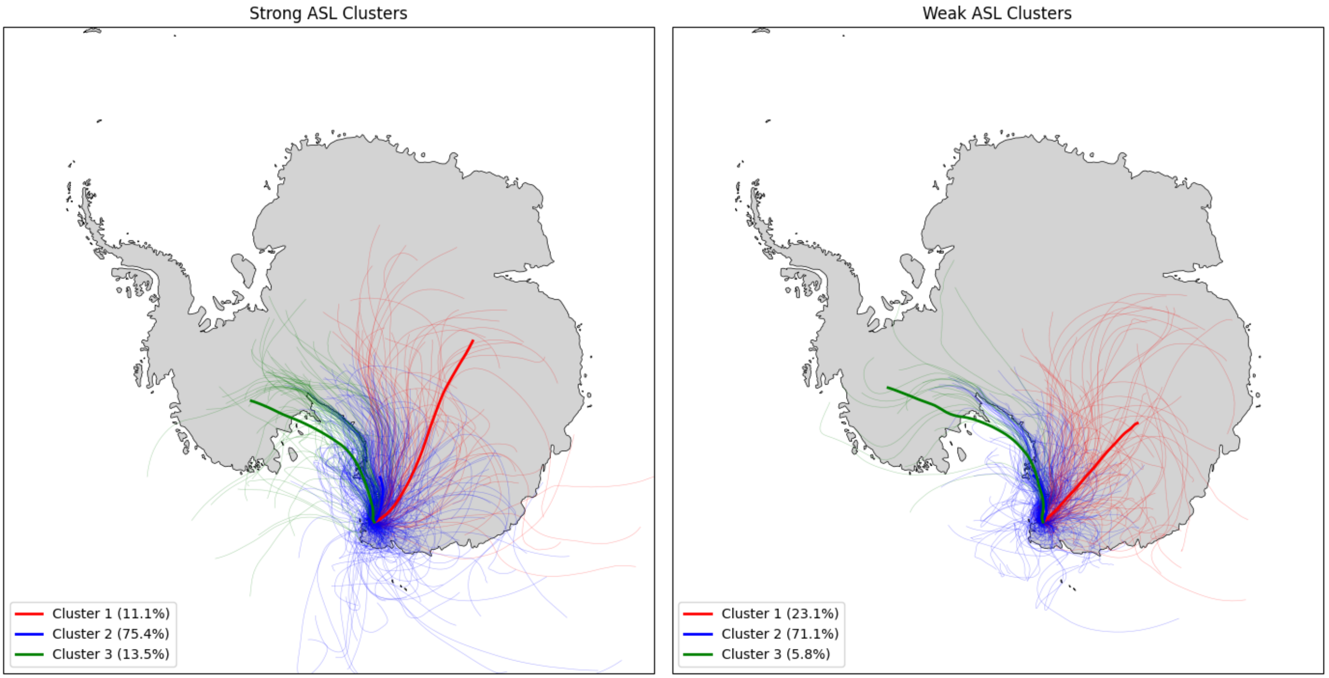

520 **Figure 7. 7-day HYSPLIT back-trajectory clusters arriving at Hercules Névé during (left) the five strongest ASL summers and (right) the five weakest ASL summers (DJF, 1979–2015). Strong ASL cases show dominant air mass transport from inland Antarctica and the Ross Ice Shelf, while weak ASL cases are associated with zonal trajectories originating from the Amundsen Sea and lower-latitude ocean sectors.**

Table 1. PCA loadings of ASL parameters (Actual central pressure, latitude, longitude) from Hosking et al. (2013) datasets. Loadings show variable contributions to each principal component.

Variable	PC1	PC2	PC3
ActCenPres (strength)	0.52	0.69	0.50
Longitude	0.50	–0.73	0.47
Latitude	0.69	0.01	–0.72

References

Bertler, N. A. N., Mayewski, P. A., and Carter, L.: Cold conditions in Antarctica during the Little Ice Age — Implications for abrupt climate change mechanisms, Earth and Planetary Science Letters, 308, 41–51, https://doi.org/10.1016/j.epsl.2011.05.021, 2011.

Casado, M., Landais, A., Picard, G., Münch, T., Laepple, T., Stenni, B., Dreossi, G., Ekaykin, A., Arnaud, L., Genthon, C., Touzeau, A., Masson-Delmotte, V., and Jouzel, J.: Archival processes of the water stable isotope signal in East Antarctic ice cores, The Cryosphere, 12, 1745–1766, https://doi.org/10.5194/tc-12-1745-2018, 2018.

Casado, M., Landais, A., Picard, G., Arnaud, L., Dreossi, G., Stenni, B., and Prié, F.: Water Isotopic Signature of Surface Snow Metamorphism in Antarctica, Geophysical Research Letters, 48, e2021GL093382, https://doi.org/10.1029/2021GL093382, 2021.

Clem, K. R., Renwick, J. A., and McGregor, J.: Large-Scale Forcing of the Amundsen Sea Low and Its Influence on Sea Ice and West Antarctic Temperature, Journal of Climate, https://doi.org/10.1175/JCLI-D-16-0891.1, 2017.

Coggins, J. H. J. and McDonald, A. J.: The influence of the Amundsen Sea Low on the winds in the Ross Sea and surroundings: Insights from a synoptic climatology, JGR Atmospheres, 120, 2167–2189, https://doi.org/10.1002/2014JD022830, 2015.

Cohen, L., Dean, S., and Renwick, J.: Synoptic Weather Types for the Ross Sea Region, Antarctica, Journal of Climate, 26, 636–649, https://doi.org/10.1175/JCLI-D-11-00690.1, 2013.

Craig, H.: Isotopic Variations in Meteoric Waters, Science, 133, 1702–1703, https://doi.org/10.1126/science.133.3465.1702, 1961.

Dale, E. R., Katurji, M., McDonald, A. J., Voss, P., Rack, W., and Seto, D.: A Comparison of AMPS Forecasts Near the Ross Sea Polynya With Controlled Meteorological Balloon Observations, JGR Atmospheres, 125, e2019JD030591, https://doi.org/10.1029/2019JD030591, 2020.

Dansgaard, W.: Stable isotopes in precipitation, Tellus, 16, 436–468, https://doi.org/10.1111/j.2153-3490.1964.tb00181.x, 1964.

Davrinche, C., Orsi, A., Agosta, C., Amory, C., and Kittel, C.: Understanding the drivers of near-surface winds in Adélie Land, East Antarctica, The Cryosphere, 18, 2239–2256, https://doi.org/10.5194/tc-18-2239-2024, 2024.

Emanuelsson, B. D., Renwick, J. A., Bertler, N. A. N., Baisden, W. T., and Thomas, E. R.: The role of large-scale drivers in the Amundsen Sea Low variability and associated changes in water isotopes from the Roosevelt Island ice core, Antarctica, Clim Dyn, 60, 4145–4155, https://doi.org/10.1007/s00382-022-06568-8, 2023.

Faber, A.-K., Møllesøe Vinther, B., Sjolte, J., and Anker Pedersen, R.: How does sea ice influence δ18O of Arctic precipitation?, Atmospheric Chemistry and Physics, 17, 5865–5876, https://doi.org/10.5194/acp-17-5865-2017, 2017.

Fernandoy, F., Meyer, H., Oerter, H., Wilhelms, F., Graf, W., and Schwander, J.: Temporal and spatial variation of stable-isotope ratios and accumulation rates in the hinterland of Neumayer station, East Antarctica, Journal of Glaciology, 56, 673–687, https://doi.org/10.3189/002214310793146296, 2010.

Frezzotti, M., Urbini, S., Proposito, M., Scarchilli, C., and Gandolfi, S.: Spatial and temporal variability of surface mass balance near Talos Dome, East Antarctica, Journal of Geophysical Research: Earth Surface, 112, https://doi.org/10.1029/2006JF000638, 2007.

Gat, J. R., Klein, B., Kushnir, Y., Roether, W., Wernli, H., Yam, R., and Shemesh, A.: Isotope composition of air moisture over the Mediterranean Sea: an index of the air-sea interaction pattern, Tellus B, 55, 953–965, https://doi.org/10.1034/j.1600-0889.2003.00081.x, 2003.

Goursaud, S., Masson-Delmotte, V., Favier, V., Orsi, A., and Werner, M.: Water stable isotope spatio-temporal variability in Antarctica in 1960–2013: observations and simulations from the ECHAM5-wiso atmospheric general circulation model, Climate of the Past, 14, 923–946, https://doi.org/10.5194/cp-14-923-2018, 2018.

Goyal, R., Jucker, M., Gupta, A. S., and England, M. H.: A New Zonal Wave-3 Index for the Southern Hemisphere, https://doi.org/10.1175/JCLI-D-21-0927.1, 2022.

Han, Y., Jun, S. J., Miyahara, M., Lee, H.-G., Ahn, J., Chung, J. W., Hur, S. D., and Hong, S. B.: Shallow ice-core drilling on Styx glacier, northern Victoria Land, Antarctica in the 2014-2015 summer, jgsk, 51, 343, https://doi.org/10.14770/jgsk.2015.51.3.343, 2015.

Hersbach, H., Bell, B., Berrisford, P., Hirahara, S., Horányi, A., Muñoz-Sabater, J., Nicolas, J., Peubey, C., Radu, R., Schepers, D., Simmons, A., Soci, C., Abdalla, S., Abellan, X., Balsamo, G., Bechtold, P., Biavati, G., Bidlot, J., Bonavita, M., De Chiara, G., Dahlgren, P., Dee, D., Diamantakis, M., Dragani, R., Flemming, J., Forbes, R., Fuentes, M., Geer, A., Haimberger, L., Healy, S., Hogan, R. J., Hólm, E., Janisková, M., Keeley, S., Laloyaux, P., Lopez, P., Lupu, C., Radnoti, G., de Rosnay, P., Rozum, I., Vamborg, F., Villaume, S., and Thépaut, J.-N.: The ERA5 global reanalysis, Quarterly Journal of the Royal Meteorological Society, 146, 1999–2049, https://doi.org/10.1002/qj.3803, 2020.

Holme, C. T., Gkinis, V., and Vinther, B. M.: Molecular diffusion of stable water isotopes in polar firn as a proxy for past temperatures, Geochimica et Cosmochimica Acta, 225, 128–145, https://doi.org/10.1016/j.gca.2018.01.015, 2018.

Hosking, J. S., Orr, A., Marshall, G. J., Turner, J., and Phillips, T.: The Influence of the Amundsen–Bellingshausen Seas Low on the Climate of West Antarctica and Its Representation in Coupled Climate Model Simulations, Journal of Climate, https://doi.org/10.1175/JCLI-D-12-00813.1, 2013.

Hwang, H., Hur, S. D., Lee, J., Han, Y., Hong, S., and Motoyama, H.: Plutonium fallout reconstructed from an Antarctic Plateau snowpack using inductively coupled plasma sector field mass spectrometry, Science of The Total Environment, 669, 505–511, https://doi.org/10.1016/j.scitotenv.2019.03.105, 2019.

Jackson, S. L., Vance, T. R., Crockart, C., Moy, A., Plummer, C., and Abram, N. J.: Climatology of the Mount Brown South ice core site in East Antarctica: implications for the interpretation of a water isotope record, Climate of the Past, 19, 1653–1675, https://doi.org/10.5194/cp-19-1653-2023, 2023.

Johnsen, S. J., Dahl-Jensen, D., Gundestrup, N., Steffensen, J. P., Clausen, H. B., Miller, H., Masson-Delmotte, V., Sveinbjörnsdottir, A. E., and White, J.: Oxygen isotope and palaeotemperature records from six Greenland ice-core stations: Camp Century, Dye-3, GRIP, GISP2, Renland and NorthGRIP, J Quaternary Science, 16, 299–307, https://doi.org/10.1002/jqs.622, 2001.

Jouzel, J., Alley, R. B., Cuffey, K. M., Dansgaard, W., Grootes, P., Hoffmann, G., Johnsen, S. J., Koster, R. D., Peel, D., Shuman, C. A., Stievenard, M., Stuiver, M., and White, J.: Validity of the temperature reconstruction from water isotopes in ice cores, J. Geophys. Res., 102, 26471–26487, https://doi.org/10.1029/97JC01283, 1997.

Kanthanathan, M., Meloth, T., Ejaz, T., Redkar, B. L., and Madhavanpillai, L. C.: Spatial distribution and post-depositional diffusion of stable waterisotopes in East Antarctica, https://doi.org/10.5194/tc-2020-77, 7 April 2020.

Kim, S., Han, C., Moon, J., Han, Y., Hur, S. D., and Lee, J.: An optimal strategy for determining triple oxygen isotope ratios in natural water using a commercial cavity ring-down spectrometer, Geosci J, 26, 637–647, https://doi.org/10.1007/s12303-022-0009-y, 2022.

Kurosaki, Y., Matoba, S., Iizuka, Y., Niwano, M., Tanikawa, T., Ando, T., Hori, A., Miyamoto, A., Fujita, S., and Aoki, T.: Reconstruction of Sea Ice Concentration in Northern Baffin Bay Using Deuterium Excess in a Coastal Ice Core From the Northwestern Greenland Ice Sheet, Journal of Geophysical Research: Atmospheres, 125, e2019JD031668, https://doi.org/10.1029/2019JD031668, 2020.

Laepple, T., Münch, T., Hirsch, N., Shaw, F., and Hörhold, M.: Limitations of ice cores in reconstructing temperature seasonality, Nature, 637, E1–E6, https://doi.org/10.1038/s41586-024-08181-7, 2025.

Maggi, V. and Petit, J.-R.: Atmospheric dust concentration record from the Hercules Névé firn core, northern Victoria Land, Antarctica, A. Glaciology., 27, 355–359, https://doi.org/10.3189/S0260305500017729, 1998.

Markle, B. R. and Steig, E. J.: Improving temperature reconstructions from ice-core water-isotope records, Clim. Past, 18, 1321–1368, https://doi.org/10.5194/cp-18-1321-2022, 2022.

Markle, B. R., Bertler, N. a. N., Sinclair, K. E., and Sneed, S. B.: Synoptic variability in the Ross Sea region, Antarctica, as seen from back-trajectory modeling and ice core analysis, Journal of Geophysical Research: Atmospheres, 117, https://doi.org/10.1029/2011JD016437, 2012.

Masson-Delmotte, V., Delmotte, M., Morgan, V., Etheridge, D., van Ommen, T., Tartarin, S., and Hoffmann, G.: Recent southern Indian Ocean climate variability inferred from a Law Dome ice core: new insights for the interpretation of coastal Antarctic isotopic records, Climate Dynamics, 21, 153–166, https://doi.org/10.1007/s00382-003-0321-9, 2003.

Masson-Delmotte, V., Hou, S., Ekaykin, A., Jouzel, J., Aristarain, A., Bernardo, R. T., Bromwich, D., Cattani, O., Delmotte, M., Falourd, S., Frezzotti, M., Gallée, H., Genoni, L., Isaksson, E., Landais, A., Helsen, M. M., Hoffmann, G., Lopez, J., Morgan, V., Motoyama, H., Noone, D., Oerter, H., Petit, J. R., Royer, A., Uemura, R., Schmidt, G. A., Schlosser, E., Simões, J. C., Steig, E. J., Stenni, B., Stievenard, M., Van Den Broeke, M. R., Van De Wal, R. S. W., Van De Berg, W. J., Vimeux, F., and White, J. W. C.: A Review of Antarctic Surface Snow Isotopic Composition: Observations, Atmospheric Circulation, and Isotopic Modeling*, Journal of Climate, 21, 3359–3387, https://doi.org/10.1175/2007JCLI2139.1, 2008.

Merlivat, L. and Jouzel, J.: Global climatic interpretation of the deuterium-oxygen 18 relationship for precipitation, J. Geophys. Res., 84, 5029–5033, https://doi.org/10.1029/JC084iC08p05029, 1979.

Münch, T., Kipfstuhl, S., Freitag, J., Meyer, H., and Laepple, T.: Regional climate signal vs. local noise: a two-dimensional viewof water isotopes in Antarctic firn at Kohnen Station, Dronning MaudLand, Clim. Past, 12, 1565–1581, https://doi.org/10.5194/cp-12-1565-2016, 2016.

Nardin, R., Amore, A., Becagli, S., Caiazzo, L., Frezzotti, M., Severi, M., Stenni, B., and Traversi, R.: Volcanic Fluxes Over the Last Millennium as Recorded in the Gv7 Ice Core (Northern Victoria Land, Antarctica), Geosciences, 10, 38, https://doi.org/10.3390/geosciences10010038, 2020.

Noone, D. and Simmonds, I.: Associations between δ18O of Water and Climate Parameters in a Simulation of Atmospheric Circulation for 1979–95, JOURNAL OF CLIMATE, 15, 2002.

Noone, D. and Simmonds, I.: Sea ice control of water isotope transport to Antarctica and implications for ice core interpretation, Journal of Geophysical Research: Atmospheres, 109, https://doi.org/10.1029/2003JD004228, 2004.

Nyamgerel, Y., Han, Y., Kim, S., Hong, S.-B., Lee, J., and Hur, S. D.: Chronological characteristics for snow accumulation on Styx Glacier in northern Victoria Land, Antarctica, J. Glaciol., 66, 916–926, https://doi.org/10.1017/jog.2020.53, 2020.

Nyamgerel, Y., Han, Y., Hwang, H., Han, C., Hong, S.-B., Do Hur, S., and Lee, J.: Climate-related variabilities in the Styx-M ice core record from northern Victoria Land, East Antarctica, during 1979–2014, Science of The Total Environment, 935, 173319, https://doi.org/10.1016/j.scitotenv.2024.173319, 2024.

Pfahl, S. and Sodemann, H.: What controls deuterium excess in global precipitation?, Clim. Past, 10, 771–781, https://doi.org/10.5194/cp-10-771-2014, 2014.

Raphael, M. N.: The influence of atmospheric zonal wave three on Antarctic sea ice variability, Journal of Geophysical Research: Atmospheres, 112, https://doi.org/10.1029/2006JD007852, 2007.

Raphael, M. N., Marshall, G. J., Turner, J., Fogt, R. L., Schneider, D., Dixon, D. A., Hosking, J. S., Jones, J. M., and Hobbs, W. R.: The Amundsen Sea Low: Variability, Change, and Impact on Antarctic Climate, Bulletin of the American Meteorological Society, 97, 111–121, https://doi.org/10.1175/BAMS-D-14-00018.1, 2016.

Raphael, M. N., Holland, M. M., Landrum, L., and Hobbs, W. R.: Links between the Amundsen Sea Low and sea ice in the Ross Sea: seasonal and interannual relationships, Clim Dyn, 52, 2333–2349, https://doi.org/10.1007/s00382-018-4258-4, 2019.

Risi, C., Bony, S., Vimeux, F., and Jouzel, J.: Water-stable isotopes in the LMDZ4 general circulation model: Model evaluation for present-day and past climates and applications to climatic interpretations of tropical isotopic records, J. Geophys. Res., 115, 2009JD013255, https://doi.org/10.1029/2009JD013255, 2010.

Scarchilli, C., Frezzotti, M., and Ruti, P. M.: Snow precipitation at four ice core sites in East Antarctica: provenance, seasonality and blocking factors, Clim Dyn, 37, 2107–2125, https://doi.org/10.1007/s00382-010-0946-4, 2011.

Schlosser, E., Stenni, B., Valt, M., Cagnati, A., Powers, J. G., Manning, K. W., Raphael, M., and Duda, M. G.: Precipitation and synoptic regime in two extreme years 2009 and 2010 at Dome C, Antarctica – implications for ice core interpretation, Atmospheric Chemistry and Physics, 16, 4757–4770, https://doi.org/10.5194/acp-16-4757-2016, 2016.

Servettaz, A. P. M., Orsi, A. J., Curran, M. A. J., Moy, A. D., Landais, A., Agosta, C., Winton, V. H. L., Touzeau, A., McConnell, J. R., Werner, M., and Baroni, M.: Snowfall and Water Stable Isotope Variability in East Antarctica Controlled by Warm Synoptic Events, JGR Atmospheres, 125, e2020JD032863, https://doi.org/10.1029/2020JD032863, 2020.

Sigl, M., Fudge, T. J., Winstrup, M., Cole-Dai, J., Ferris, D., McConnell, J. R., Taylor, K. C., Welten, K. C., Woodruff, T. E., Adolphi, F., Bisiaux, M., Brook, E. J., Buizert, C., Caffee, M. W., Dunbar, N. W., Edwards, R., Geng, L., Iverson, N., Koffman, B., Layman, L., Maselli, O. J., McGwire, K., Muscheler, R., Nishiizumi, K., Pasteris, D. R., Rhodes, R. H., and Sowers, T. A.: The WAIS Divide deep ice core WD2014 chronology – Part 2: Annual-layer counting (0–31 ka BP), Climate of the Past, 12, 769–786, https://doi.org/10.5194/cp-12-769-2016, 2016.

Sime, L., Wolff, E., Oliver, K., and Tindall, J.: Evidence for warmer interglacials in East Antarctic ice cores, Nature, 462, 342–345, https://doi.org/10.1038/nature08564, 2009.

Sinclair, K. E., Bertler, N. A. N., and Ommen, T. D. van: Twentieth-Century Surface Temperature Trends in the Western Ross Sea, Antarctica: Evidence from a High-Resolution Ice Core, https://doi.org/10.1175/JCLI-D-11-00496.1, 2012.

Sinclair, K. E., Bertler, N. A. N., Trompetter, W. J., and Baisden, W. T.: Seasonality of Airmass Pathways to Coastal Antarctica: Ramifications for Interpreting High-Resolution Ice Core Records, Journal of Climate, 26, 2065–2076, https://doi.org/10.1175/JCLI-D-12-00167.1, 2013.

Song, W., Liu, Z., Lan, H., and Huan, X.: Influence of seasonal sea-ice loss on Arctic precipitation δ18O: a GCM-based analysis of monthly data, Polar Research, 42, https://doi.org/10.33265/polar.v42.9751, 2023.

Stammerjohn, S. E., Maksym, T., Massom, R. A., Lowry, K. E., Arrigo, K. R., Yuan, X., Raphael, M., Randall-Goodwin, E., Sherrell, R. M., and Yager, P. L.: Seasonal sea ice changes in the Amundsen Sea, Antarctica, over the period of 1979–2014, Elementa: Science of the Anthropocene, 3, 000055, https://doi.org/10.12952/journal.elementa.000055, 2015.

Steig, E. J., Morse, D. L., Waddington, E. D., Stuiver, M., Grootes, P. M., Mayewski, P. A., Twickler, M. S., and Whitlow, S. I.: Wisconsinan and Holocene Climate History from an Ice Core at Taylor Dome, Western Ross Embayment, Antarctica, Geografiska Annaler: Series A, Physical Geography, 82, 213–235, https://doi.org/10.1111/j.0435-3676.2000.00122.x, 2000.

Stein, A. F., Draxler, R. R., Rolph, G. D., Stunder, B. J. B., Cohen, M. D., and Ngan, F.: NOAA's HYSPLIT Atmospheric Transport and Dispersion Modeling System, Bulletin of the American Meteorological Society, 96, 2059–2077, https://doi.org/10.1175/BAMS-D-14-00110.1, 2015.

Stenni, B., Caprioli, R., Cimino, L., Cremisini, C., Flora, O., Gragnani, R., Longinelli, A., Maggi, V., and Torcini, S.: 200 years of isotope and chemical records in a firn core from Hercules Névé, northern Victoria Land, Antarctica, Ann. Glaciol., 29, 106–112, https://doi.org/10.3189/172756499781821175, 1999.

Stenni, B., Serra, F., Frezzotti, M., Maggi, V., Traversi, R., Becagli, S., and Udisti, R.: Snow accumulation rates in northern Victoria Land, Antarctica, by firn-core analysis, Journal of Glaciology, 2000.

Stenni, B., Proposito, M., Gragnani, R., Flora, O., Jouzel, J., Falourd, S., and Frezzotti, M.: Eight centuries of volcanic signal and climate change at Talos Dome (East Antarctica), Journal of Geophysical Research: Atmospheres, 107, ACL 3-1-ACL 3-13, https://doi.org/10.1029/2000JD000317, 2002.

Tetzner, D., Thomas, E., and Allen, C.: A Validation of ERA5 Reanalysis Data in the Southern Antarctic Peninsula—Ellsworth Land Region, and Its Implications for Ice Core Studies, Geosciences, 9, 289, https://doi.org/10.3390/geosciences9070289, 2019.

Tewari, K., Mishra, S. K., Dewan, A., and Ozawa, H.: Effects of the Antarctic elevation on the atmospheric circulation, Theor Appl Climatol, 143, 1487–1499, https://doi.org/10.1007/s00704-020-03456-1, 2021.

Thomas, E. R., van Wessem, J. M., Roberts, J., Isaksson, E., Schlosser, E., Fudge, T. J., Vallelonga, P., Medley, B., Lenaerts, J., Bertler, N., van den Broeke, M. R., Dixon, D. A., Frezzotti, M., Stenni, B., Curran, M., and Ekaykin, A. A.: Regional Antarctic snow accumulation over the past 1000 years, Climate of the Past, 13, 1491–1513, https://doi.org/10.5194/cp-13-1491-2017, 2017.

Turner, J., Phillips, T., Hosking, J. S., Marshall, G. J., and Orr, A.: The Amundsen Sea low, Intl Journal of Climatology, 33, 1818–1829, https://doi.org/10.1002/joc.3558, 2013.

Turner, J., Hosking, J. S., Marshall, G. J., Phillips, T., and Bracegirdle, T. J.: Antarctic sea ice increase consistent with intrinsic variability of the Amundsen Sea Low, Clim Dyn, 46, 2391–2402, https://doi.org/10.1007/s00382-015-2708-9, 2016.

Uemura, R., Matsui, Y., Yoshimura, K., Motoyama, H., and Yoshida, N.: Evidence of deuterium excess in water vapor as an indicator of ocean surface conditions, J. Geophys. Res., 113, 2008JD010209, https://doi.org/10.1029/2008JD010209, 2008.

Vihma, T., Tuovinen, E., and Savijärvi, H.: Interaction of katabatic winds and near-surface temperatures in the Antarctic: KATABATIC WINDS IN THE ANTARCTIC, J. Geophys. Res., 116, https://doi.org/10.1029/2010jd014917, 2011.

Yan, Y., Spaulding, N. E., Bender, M. L., Brook, E. J., Higgins, J. A., Kurbatov, A. V., and Mayewski, P. A.: Enhanced moisture delivery into Victoria Land, East Antarctica, during the early Last Interglacial: implications for West Antarctic Ice Sheet stability, Climate of the Past, 17, 1841–1855, https://doi.org/10.5194/cp-17-1841-2021, 2021.

Yang, J., Han, Y., Orsi, A. J., Kim, S., Han, H., Ryu, Y., Jang, Y., Moon, J., Choi, T., Hur, S. D., and Ahn, J.: Surface Temperature in Twentieth Century at the Styx Glacier, Northern Victoria Land, Antarctica, From Borehole Thermometry, Geophysical Research Letters, 45, 9834–9842, https://doi.org/10.1029/2018GL078770, 2018.